INTERNATIONAL JOURNAL OF HYDROGEN ENERGY XXX (2018) 1–12

Available online at www.sciencedirect.com

ScienceDirect

journal homepage: www.elsevier.com/locate/he

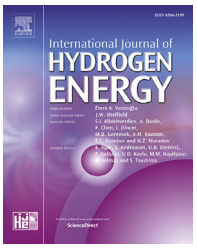

Direct injection internal combustion engine with high-pressure thermochemical recuperation – Experimental study of the first prototype

A. Poran [a], A. Thawko [a], A. Eyal [b], L. Tartakovsky [a,b,*]

[a] Grand Technion Energy Program, Technion – Israel Institute of Technology, Technion City, Haifa 3200003, IL, Israel
[b] Faculty of Mechanical Engineering, Technion – Israel Institute of Technology, Technion City, Haifa 3200003, IL, Israel

ARTICLE INFO

Article history:
Received 24 February 2018
Received in revised form
22 April 2018
Accepted 24 April 2018
Available online xxx

Keywords:
Waste heat recovery
Thermochemical recuperation
Hydrogen
Internal combustion engine
Methanol steam reforming
Gas direct injection

ABSTRACT

The paper describes, for the first time, experimental study results of a novel direct-injection (DI) internal combustion engine (ICE) with high-pressure thermochemical recuperation (HP-TCR) fed by methanol as a primary fuel. The reported system is the first ever working prototype of ICE with HP-TCR. A detailed description of the developed novel technology, physical and chemical processes in the system is presented. HP-TCR system performance is discussed and compared to the previously published study results of the same engine fed with artificially prepared reformate from compressed gas cylinder. HP-TCR demonstrates a significant improvement over the gasoline reference case with 19% –30% relative increase in indicated efficiency and reduction in NO_x, CO, HC and CO_2 emissions by up to 97, 91, 96 and 15%, respectively. The system performance shows a good prospect to continue the research towards an automotive-scale system development. Further performance improvement options are discussed as well.

Introduction

Internal combustion engines (ICE) are a major fossil oil consumption and environmental pollution source. Hence, pollutant and greenhouse gas (GHG) emissions mitigation and petroleum utilization reduction can be achieved by increasing the ICE efficiency and using alternative low-carbon-intensity fuels [1]. Ethanol and methanol are widely investigated as alternative fuels since they have low carbon content [2–4]. Methanol has an advantage because it can be produced from both fossil and renewable sources such as natural gas, coal, bio-mass, and renewable energy-derived hydrogen.

In an ICE, about 30% of the fuel energy is wasted along with the hot exhaust gas [5,6]. Thus, methods that partially utilize this energy, also known as waste heat recovery (WHR) methods, are widely investigated nowadays and may contribute significantly to the overall ICE efficiency

* *Corresponding author*. Faculty of Mechanical Engineering, Grand Technion Energy Program, Technion – Israel Institute of Technology, Technion City, Haifa 3200003, Israel.
E-mail address: tartak@technion.ac.il (L. Tartakovsky).

https://doi.org/10.1016/j.ijhydene.2018.04.190
0360-3199/

Nomenclature

Symbols

δR	uncertainty of calculated parameter R
δX_i	accuracy of measured value X_i
ΔH	enthalpy of reaction
E_i	emissions of pollutant i
F	methanol conversion fraction
$\overline{h}_{add}$	normalized added enthalpy to the reformate
$\overline{h}_{av}$	normalized enthalpy available for reforming
h_f	fuel enthalpy
K	dry to wet molar ratio of the exhaust gas
$\dot{m}_f$	fuel mass flow rate
M_C	molecular weight of carbon
$M_{exh.w}$	molecular weight of wet exhaust gas
M_i	molecular weight of pollutant i
$\dot{n}_{c,exh}$	carbon molar flow rate in the exhaust gas
$\dot{n}_M$	methanol molar flow rate from the pump
p	cylinder pressure
T_{ev}	water-methanol mixture evaporation temperature
V	cylinder volume
V_d	displaced volume
$W_{i,g}$	gross indicated work
$P_{i,g}$	gross indicated power
$y_{c,fuel}$	fuel's carbon mass fraction
y_i	molar fraction of pollutant i
y_j	CO/CO_2/$CH_{1.85}$ M fraction

Greek symbols

E	heat exchanger effectiveness factor
η_i	gross indicated efficiency
λ	excess air ratio

Acronyms

BTE	brake thermal efficiency
DI	direct injection
ED	ethanol decomposition
GC	gas chromatograph
HC	hydrocarbons
HE	heat exchanger
HP-TCR	high-pressure thermochemical recuperation
ICE	internal combustion engine
IMEP	indicated mean effective pressure (gross)
LHV	lower heating value
MD	methanol decomposition
MSR	methanol steam reforming
MWM	methanol-water mixture
SI	spark ignition
STP	standard temperature and pressure
TCR	thermochemical recuperation
WHR	waste heat recovery

improvement [7–11]. The WHR method that utilizes the exhaust gas energy to sustain endothermic fuel reforming reactions is called thermochemical recuperation (TCR) [6,12,13]. TCR has two main advantages over other WHR methods. It increases the fuel lower heating value (LHV) due to the WHR through endothermic fuel reforming reactions — Eqs. (1) and (2), and allows onboard hydrogen-rich reformate production with its subsequent combustion. The latter results in an increased burning velocity, higher knock resistance and wider flammability limits [14,15]. Thus, TCR contributes to the ICE efficiency improvement not only due to the WHR but also because of lean-burn operating possibilities, combustion that closer approximates the ideal Otto cycle and the possibility of increasing the engine compression ratio [16].

In the reported study, we employed methanol as a primary fuel for a propulsion system with waste heat recovery (WHR) through High-Pressure Thermochemical Recuperation (HP-TCR). In addition to its previously mentioned advantages, methanol is also an excellent primary fuel for TCR since it can be reformed at relatively low temperatures (approximately 250–300 °C) to produce hydrogen-rich reformate. The widely investigated methanol reforming reactions for ICE applications are methanol decomposition — MD (Eq. (1)) and methanol steam reforming — MSR (Eq. (2)), [16–19].

$$CH_3OH_{(g)} \rightarrow CO + 2H_2 \quad \Delta H = 90\ kJ/mol \tag{1}$$

$$CH_3OH_{(g)} + H_2O_{(g)} \rightarrow CO_2 + 3H_2 \quad \Delta H = 50\ kJ/mol \tag{2}$$

Methanol exhaust gas reforming is considered by some researchers as well [4,16,20]. It comprises of steam- (Eq. (2)) and dry-reforming endothermic reactions accompanied by some exothermic fuel oxidation due to air presence in the exhaust gas. In exhaust gas reforming a part of the heat required for endothermic steam and dry reforming is supplied by partial or full oxidation reactions. Evidently, waste heat recuperation potential of this method is lower compared to MSR and MD.

In this research, the MSR method was chosen due to available experimental data showing good catalyst stability at high pressures [21]. Notably, MD has some advantages over MSR since there is no need to carry, preheat, and evaporate water in the reforming system; a higher WHR rate can be achieved, and a reformate with higher heating value is produced. The latter enables using lower injection pressure in the case of direct injection. Unfortunately, catalyst stability and deactivation problems are reported for MD mainly due to coke formation [22]. In case the newly developed MD catalysts as reported in Ref. [23] will show good stability at high pressures, this may be the preferred reforming method. Conversely, an advantage of MSR over MD is that the presence of CO_2 in the reformate (constitutes 17% wt. of a stoichiometric MSR reformate-air mixture) leads to decrease of the in-cylinder combustion temperatures and thus results in a significant reduction in NO_x emission.

Methanol reforming has been thoroughly investigated in the past. Even a vehicle with an on-board reformer was built and demonstrated up to 40% brake thermal efficiency (BTE) improvement compared to the baseline gasoline engine [18]. However, problems such as catalyst deactivation, uncontrolled combustion, cold start, and engine maximal power loss due to reduced volumetric efficiency were also reported [18]. Volumetric efficiency reduction and uncontrolled combustion occurred as a result of supplying the reformate through the intake manifold. The hydrogen-rich reformate reduced the

Please cite this article in press as: Poran A, et al., Direct injection internal combustion engine with high-pressure thermochemical recuperation – Experimental study of the first prototype, International Journal of Hydrogen Energy (2018), https://doi.org/10.1016/j.ijhydene.2018.04.190

specific volume of air in the intake manifold and thus less air ingested to the cylinders in the intake stroke. A commonly employed solution of the reduced maximal power and uncontrolled combustion problems is to limit the reformate usage percentage at medium-low loads and to combust the primary non-reformed fuel at high loads [18]. More recent studies resolved the uncontrolled combustion and reduced maximal power issues in a hydrogen-fueled ICE by direct injection (DI) of the hydrogen into the cylinder rather than into the intake manifold [24]. Integrating the ICE-TCR system into a series hybrid electric propulsion was suggested to overcome the cold start and transient behavior challenges (a battery or super-capacitor could be used as an energy source for cold start) [25].

In a previous study, we suggested to harness the advantages of hydrogen DI ICE with the benefits of TCR and showed that performing the reforming reactions at high pressure is essential to enable direct injection of the reformate into the engine cylinders [26]. Otherwise, the amount of energy necessary to compress the gaseous reformate from atmospheric pressure prior to its injection would consume a significant fraction of the engine power and make this approach infeasible. Thus, the concept of HP-TCR (with a liquid- instead of a gas compression) was introduced. A simulation of ICE with HP-TCR system based on methanol steam reforming showed a BTE improvement of 14% compared to the gasoline-fed counterpart. The promising simulation results served as a basis for the subsequent experimental study [27–29].

As a first experimental step, a DI ICE fueled with artificially prepared MSR products ($0.25CO_2$ and $0.75H_2$ mole fractions) from the compressed gas cylinder was developed and investigated. It showed 18%–39% increase in indicated efficiency and reduction of 73–94%, 90–96%, 85–97%, 10–25% in NO_x, CO, HC and CO_2 emissions, respectively, compared with the gasoline baseline engine in a wide power range [27]. Further investigation showed an importance of reformate injection strategy and especially end-of-injection event on engine efficiency and pollutant emissions [28]. To improve energy utilization, the primary fuel pre-heating by a hot reformate was suggested [28]. An importance of this approach as an efficient method of exergy destruction minimization was confirmed later by Chuahy & Kokjohn [30].

In the research reported in this article, the previously developed laboratory engine was coupled with a high-pressure methanol steam reforming reactor to form the first ICE with HP-TCR system ever built. The ICE with HP-TCR was proven to work successfully at different steady-state operating modes and the system performance was analyzed. Even though the measured performance of ICE with HP-TCR is good, suggestions aimed at further system improvement are discussed as well.

Methodology

Experimental setup

The experimental setup was based on a single-cylinder carburetor gasoline-fed SI engine (baseline configuration) converted to operate with direct injection of gaseous reformate. Fig. 1 shows the experimental setup scheme.

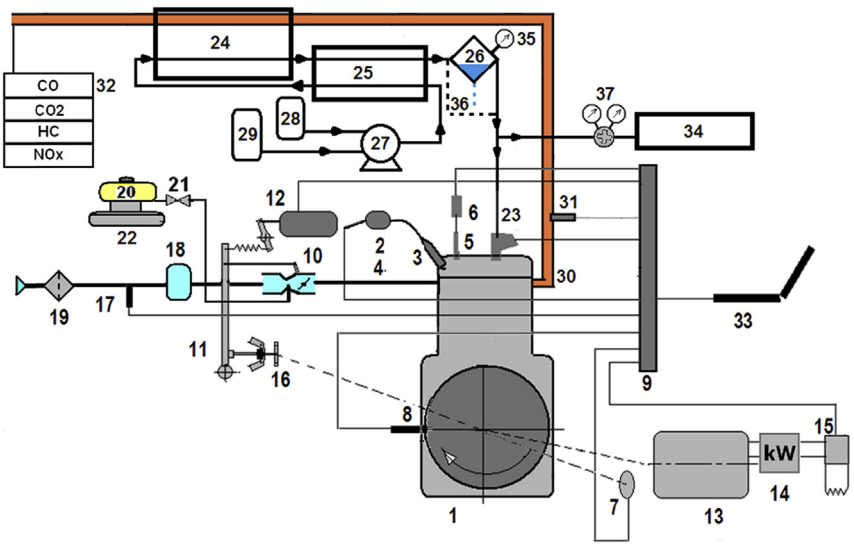

Fig. 1 – Scheme of the experimental setup. 1 – Robin EY20-3 single cylinder ICE; 2 – ignition coil; 3 – spark plug; 4 – air intake system; 5 – pressure transducer; 6 – charge amplifier; 7 – crankshaft encoder; 8 – top dead center proximity sensor; 9 – ECU and data acquisitor; 10 – throttle; 11 – centrifugal speed governor; 12 – linear actuator; 13 – generator; 14 – power gauge 15 –proportional controller; 16 – crankshaft driven gear of the engine speed governor; 17 – air flow meter; 18 – pressure wave damper; 19 – air filter; 20 – gasoline tank; 21 – valve; 22 – electronic scales; 23 – DI gas injector; 24 – reformer; 25 – heat exchanger; 26 – liquid separation tank and reformate reservoir; 27 – fuel pump; 28 – methanol tank; 29 – water tank; 30 – exhaust line; 31 – O_2 sensor; 32 – exhaust gas analyzers; 33 – computer; 34 – gas chromatograph; 35 – pressure gauge; 36 – liquid separation tank bypass; 37 – pressure regulator.

Please cite this article in press as: Poran A, et al., Direct injection internal combustion engine with high-pressure thermochemical recuperation – Experimental study of the first prototype, International Journal of Hydrogen Energy (2018), https://doi.org/10.1016/j.ijhydene.2018.04.190

The laboratory engine was based on a Robin-EY20-3 4-stroke spark ignition (SI) air-cooled, single cylinder ICE (1) coupled with a Sincro GP100 2.2 kW AC 230 V generator (13). This engine was selected as the basis for the first prototype of a DI MSR-fed engine because of the extra space in the cylinder head that enabled the relatively easy mounting of an in-house developed gas-DI injector and an in-cylinder pressure transducer. The main baseline engine parameters are listed in Table 1.

The original ICE ignition system was replaced by an AEM 30-2853 coil (2) and a Denso IWF 24 Iridium spark plug (3) to enable a spark charge and spark timing variation. Engine control and data logging were carried out with a dSPACE DS 1104 controller (9) connected to a computer (33). In-cylinder pressure and crank angle measurements were performed with a Kistler 6061B water-cooled pressure transducer (5) connected to Kistler 5018 charge amplifier (6) and a Kistler crankshaft encoder 2613B (7) at a resolution of 0.5° mounted on the free end of the generator shaft, respectively. The pressure transducer was installed in the cylinder head according to the manufacturer instructions. The engine speed was regulated by varying the spring load of the governor with a linear actuator (12) in the case of gasoline-fed operating and by changing the injected fuel quantity and load for the case of gaseous operation. The engine load was controlled via resistors and a Crydom 10PVC2425 proportional controller (15) which were connected to the gen-set generator and controlled by the ECU (9, 33). Gasoline consumption was measured by using the digital scales GF-12K from A&D Ltd. (22). Methanol and water were supplied to the heat exchanger (HE) (25) inlet by a Knauer BlueShadow P80 pump (27) equipped with a binary LPG valve that allowed setting different volumetric flow rates from the methanol and water tanks (28 & 29).

The HE (25) in which the methanol-water mixture (MWM) was pre-heated by the hot reformate effluent was a 00540-03 model shell-and-tube type with a heat transfer area of 0.11 m^2 produced by Exergy LLC. From the HE, the preheated MWM entered an in-house developed reformer (24). A schematic layout of the reformer is shown in Fig. 2.

The reformer was built from 7 tubes with a length of 860 mm and diameter 3/8″ yielding 0.18 m^2 heat transfer area. The tubes were confined in a 2″ shell and welded to flanges at the top and bottom end. Thermocouples were inserted into four of the catalyst tubes along their axis to different distances from the top cover (705, 530, 305 and 140 mm). Two more thermocouples were inserted 5 mm from the top and bottom cover. The mixture flowed down the center tube of the reformer in a 1/8″ tube and then back up in the 3/8″ evaporation tube. From the top of the evaporation tube, the mixture flowed down in 6 catalyst tubes to the reformer outlet. The catalyst tubes were filled with 430 g of commercial G-66 CuO/ZnO catalyst (cylindrical pellets of 3 mm diameter and length), courtesy of Clariant.

Table 1 – Specifications of Robin EY-20 ICE.

Bore × Stroke, mm	67 × 52
Displacement, cm^3	183
Compression ratio	6.3
Power, kW @ speed, rpm	2.2 @ 3000
Continues BMEP @ 3000 rpm, bar	4.8
Gasoline feed system	Carburetor

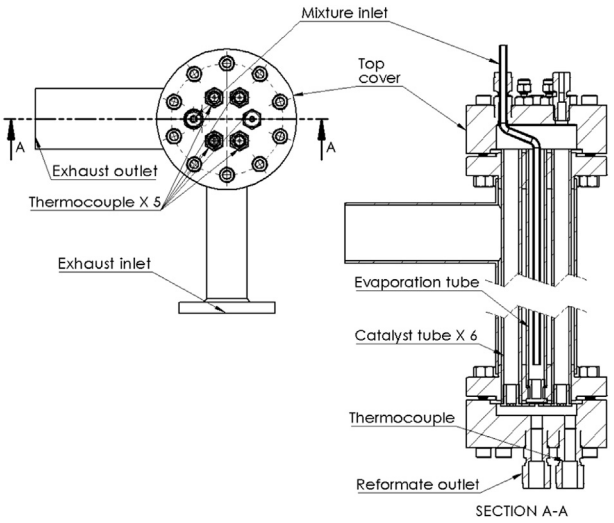

Fig. 2 – Schematic layout of the reformer.

From the reformer, the hot reformate effluent was redirected to the HE (25) to cool down and preheat the MWM supplied by the pump (27) at the controlled high pressure. The reformate was then directed either through a liquid separation tank (26) or a bypass (36) directly to the DI injector. Note that the experimental results discussed in the reported study of DI ICE with HP-TCR system is a significant step forward compared to the studies previously published by the authors of the same engine fed by artificially prepared reformate [27,28], because the developed system is the first ever working prototype of ICE with HP- TCR, which was investigated for the first time.

To measure reformate composition, a sample line was drawn from nearby the injector to an Agilent 490 micro gas chromatograph (GC) equipped with 1 m COX and 10 m PPU columns through a pressure regulator (37) and two thermal conductivity detectors (TCD). The GC was also equipped with Genie filter to remove liquids. Hence, the GC analysis includes only the dry reforming products and does not give an indication of the real amounts of water and methanol in the reformate. The chosen GC operation method allowed measuring the reformate composition every 2.5–3 min in both channels and the presented results are the average of readings in both channels. Extraction flow to the GC was set to approximately 1 l/min (at STP condition) which for MSR reformate yielded about 1–2% from the total fuel flow rate and hence was neglected in fuel consumption calculations.

CO_2 and CO concentrations were measured from a dried exhaust gas sample line with a California Analytical Instrument (CAI) 600 series NDIR analyzer. NO_x concentration was measured from the same sampling line using a Thermal Converter 501× and NO_x chemiluminescent analyzer 200 EH from Teledyne Instruments. Total hydrocarbons (HC) were measured through a heated sample line with a CAI 600 series FID HC analyzer.

Please cite this article in press as: Poran A, et al., Direct injection internal combustion engine with high-pressure thermochemical recuperation – Experimental study of the first prototype, International Journal of Hydrogen Energy (2018), https://doi.org/10.1016/j.ijhydene.2018.04.190

The intake air flow rate was measured by a VA-420 flow sensor and verified by the calculation of an exhaust gas carbon balance and by using a wide-band Lambda sensor kit LC-1 from Innovate Motorsports. The latter is based on a Bosch LSU 4.2 O_2 sensor (31).

In this study, we used an in-house-developed direct gaseous fuel injector. The injector was developed based on a commercial Magneti Marelli IHP072 gasoline DI injector. A modification was made to the nozzle to allow higher volumetric flow rates required for gaseous fuel injection. The injector flow area was 0.85 mm^2, and its discharge coefficient was in the range of 0.87 ± 0.07. Further details on the developed injector and its mounting in the engine head can be found in Refs. [28,29]. The gas DI injector location, orientation, and injection strategy optimization were beyond the scope of this work and is not discussed hereinafter.

Experimental procedure

The ICE with HP-TCR performance was investigated at steady-state. To monitor the system operation regime and be able to ensure that it achieved steady-state operation, the reformer and the engine temperatures, engine control parameters, and reforming pressure were measured and carefully monitored during the whole duration of the experiment. The system was considered to achieve steady-state operation when the average reformer temperature and pressure gradients did not exceed 0.5 K/min and 0.1 bar/min, respectively (compared to 20 K/min and 9 bar/min when the reformer is heated before reaching the steady-state). The operating regimes (various loads at constant engine speed and wide-open-throttle – WOT) were chosen based on the previous engine testing experience (Table 2) [27,28]. Ignition timing used in this study was based on MBT values measured in experiments with artificial MSR from compressed gas cylinders [27,28].

At the first two operation modes, the separation tank was used. At lower loads, it was advantageous to work with the bypass. For the lowest load studied (#7), the injection pressure was reduced and the throttle was partially closed to enable better energy extraction from the exhaust gases. The energetic considerations made during these experiments are discussed in the Section Results & Discussion.

Data processing

The measured data were processed to obtain the results as described in the following section.

The gross indicated mean effective pressure (IMEP) was calculated by integrating the in-cylinder pressure values over the cylinder volume for the compression and expansion strokes only (Eq. (3)):

$$IMEP = \frac{\int pdV}{V_d} = \frac{W_{i,g}}{V_d} \tag{3}$$

Where: V_d is the displaced volume; V is the cylinder volume; p is the cylinder pressure; $W_{i,g}$ is the gross indicated work.

The integration was performed numerically using the trapezoidal method. For every engine regime shown in this work, approximately 100 cycles were measured, and the IMEP shown is that of the average cycle for the considered regime. For the case of system-steady state operation, at least three measurements of 100 cycles each were conducted at the begging, middle and end of steady-state operation period.

The gross indicated efficiency (η_i) was calculated following Eq. (4) [31]:

$$\eta_i = \frac{P_{i,g}}{\dot{m}_f \cdot LHV_f} \tag{4}$$

Where: $P_{i,g}$ is the gross indicated power; $\dot{m}_f$ is the fuel mass flow rate; LHV_f is the fuel lower heating value (for MSR reformate, $\dot{m}_f$ and LHV_f were calculated according to the mass flow rate LHV of the consumed primary fuel – methanol).

A schematic illustration of the flow arrangement in the experimental system is shown in Fig. 3.

Temperatures were measured in points 1-5,7 & 8 and the enthalpy at these points was calculated based on the temperature measured by thermocouples (without wall temperature correction) assuming ideal gas or compressed liquid both as ideal mixtures, i.e. $h = h(T)$. The reformate normalized added enthalpy was calculated according to Eq. (5):

$$\overline{h}_{add} = \frac{\dot{m}_1(h_4 - h_1)}{\dot{m}_5 LHV_5} \tag{5}$$

Where: $\dot{m}_1$ is the MWM flow rate in the HE (25); h_4 is the specific enthalpy of reforming products at the HE outlet assuming ideal gas mixture; h_1 is the enthalpy of MWM (assuming ideal mixture) at the HE inlet; $\dot{m}_5$ is the reformate fuel mass flow rate to the engine.

Since the process between points 1 and 2 includes the MWM evaporation, there is no possibility to achieve an equality of the temperatures in points 2 and 3, whereas the temperature of the hot stream cannot be lower than T_1. Thus, the HE effectiveness was calculated according to Eq. (6):

Table 2 – Engine operating parameters at steady-state.

No.	Speed [rpm]	IMEP [bar]	Flow arrangement	Injection pressure [bar]	Excess air ratio, λ	Throttle position	COV[a]
1	2800	5.31	separation tank (26 in Fig. 1)	50	1.37	WOT	0.0157
2	2800	4.96	separation tank (26 in Fig. 1)	50	1.58	WOT	0.0240
3	2800	5.89	bypass (36 in Fig. 1)	50	1.21	WOT	0.0124
4	2800	4.38	bypass (36 in Fig. 1)	50	1.83	WOT	0.0325
5	2800	4.86	bypass (36 in Fig. 1)	50	1.62	WOT	0.0208
6	2800	5.05	bypass (36 in Fig. 1)	50	1.65	WOT	0.0340
7	2800	3.69	bypass (36 in Fig. 1)	30	1.33	Partially closed	0.0268

[a] COV – Coefficient of variation calculated according to [31].

Please cite this article in press as: Poran A, et al., Direct injection internal combustion engine with high-pressure thermochemical recuperation – Experimental study of the first prototype, International Journal of Hydrogen Energy (2018), https://doi.org/10.1016/j.ijhydene.2018.04.190

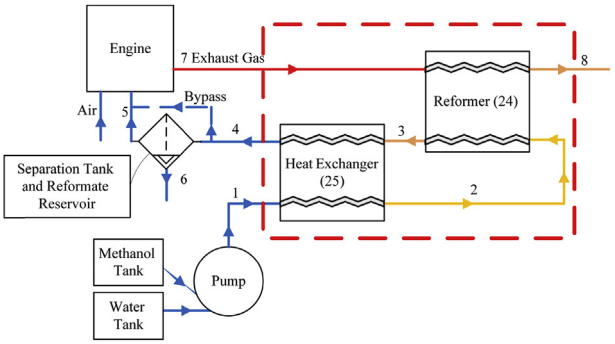

Fig. 3 – Schematic layout of the flow arrangement in the experimental setup. Numbers in the parentheses correspond to those in Fig. 1. The working fluid at various system points: 1 – MWM; 2 – pre-heated MWM; 3 – hot reformate; 4 – cooled reformate; 5 – reformate with or without condensable water and methanol; 6 – condensed water and methanol; 7 – hot exhaust gas; 8 – cooled exhaust gas.

$$\varepsilon = \frac{q}{q_{\max}} = \frac{h_3 - h_4}{h_3 - h_{ref}(T_1)} \tag{6}$$

Where: $h_{ref}(T_1)$ is the reformate enthalpy if it would have exits the HE at the temperature T_1 (i.e. ideal HE).

The normalized available exhaust gas enthalpy ($\overline{h}_{av}$) was calculated according to Eq. (7):

$$\overline{h}_{av} = \frac{\dot{m}_7(h_7 - h_8)}{\dot{m}_5 LHV_5} \tag{7}$$

Methanol conversion (f) was calculated for cases that reformate flowed through the liquid separation tank (26) using carbon balance analysis (Eq. (8)):

$$f = \frac{\dot{n}_{c,exh}}{\dot{n}_M} = \frac{K\left[\dot{m}_a\left(1 + (F/A)_{st}/\lambda\right)/M_{exh.w}\right]\left(y_{CO_2} + y_{CO} + y_{HC}/K\right)}{\dot{m}_M/M_M} \tag{8}$$

Where: $\dot{n}_{c,exh}$ is the carbon molar flow rate in the exhaust gas; $\dot{n}_M$ is the methanol molar flow rate from the pump; $\dot{m}_a$ is air mass flow rate; $M_{exh.w}$ is the molecular weight of the wet exhaust gas; K is the molar ratio between dry and wet exhaust gas; y_j is the molar fraction of species j taken from dry (CO_2 and CO) or wet (HC) exhaust sample; $\dot{m}_M$ is the methanol mass flow rate to the reformer; M_M is methanol molecular weight.

The carbon analysis method has a certain drawback because it cannot distinguish between combustion of unreformed methanol and the reformate. However, for the cases in which the liquid separation tank (26 in Fig. 1) was used, this uncertainty is small because the reformate was injected into the engine cylinder at temperature 308 K and pressure 50 bar and thus limits the amount of methanol vapor in the reformate to 0.6% mol/mol. When the bypass (36 in Fig. 1) was used, only a small amount of condensate reached the liquid separation tank – on average 4% wt. (measured as a mass of MWM accumulated in the tank divided by the total MWM mass supplied during the experiment). The reformate gas-chromatography analysis showed that the reforming products comprise much more water than methanol (due to high measured amounts of CO and CH_4 in the reformate). Also, water vapor pressure is lower than that of methanol. Thus, in efficiency calculations, a conservative assumption that there is no methanol in the condensate was used (i.e., all the supplied methanol was consumed). To estimate the combusted methanol influence (with the bypass) on the conversion value calculated according to Eq. (8), a comparison of the reformer temperature distribution and flow rates with and without the bypass was done. The correctness of the employed assumptions was also verified by a first law analysis of the control volume comprising the reformer and the HE (i.e. checking that $\overline{h}_{av} > \overline{h}_{add}$ as an upper possible limit).

The measured pollutant concentrations to specific pollutant emissions conversion (in g/kWh) was performed based on a carbon balance analysis, measured fuel flow rates and the assumption that the lube oil burn and particulate formation effects on the carbon balance are negligible (Eq. (9)).

$$E_i = \frac{\dot{m}_f \cdot y_{c,fuel} \cdot y_i \cdot M_i}{M_C \cdot \left(y_{CO_2} + y_{CO} + y_{HC}/K\right) \cdot P_{i,g}} \tag{9}$$

Where: E_i is the specific pollutant emission of pollutant i; $y_{c,fuel}$ is the fuel carbon mass fraction; y_i is the molar fraction of pollutant i; M_i is the molecular weight of pollutant i; M_C is the molecular weight of carbon.

The uncertainty of the calculated parameters was assessed using Eq. (10) [32]:

$$\delta R = \left(\sum_{i=1}^{N}\left(\frac{\partial R}{\partial X_i}\delta X_i\right)^2\right)^{1/2} \tag{10}$$

Where δR is the uncertainty of calculated parameter R; $\frac{\partial R}{\partial X_i}$ is the partial derivative of R with respect to measured value X_i; δX_i is the accuracy of the measured value X_i.

It is known that the IMEP calculation is insensitive to random noise and absolute pressure referencing errors but is very sensitive to crank phasing errors [33]. The calculation also involves numerical integration. Thus, IMEP uncertainty was calculated by applying the approach suggested by Moffat [32] for computing uncertainty when a computer program is used for the results analysis. An angle phase error of ±0.5° was used in this calculation (equal to the encoder resolution). The average IMEP uncertainty was found to be 2.1% with a maximal uncertainty of 5% that was observed at idle and engine feeding with MSR. Table 3 summarizes the accuracy of the measured data and uncertainty of the calculated parameters. The uncertainty values calculated for indicated efficiency, and NO_x, HC, CO and CO_2 emissions are shown as error bars in Figs. 9–12. In some cases, due to the wide range of values shown in one graph, error bars may not be seen due to their relatively small absolute values.

Results and discussion

The discussion section focuses on both the reforming process parameters and the whole HP-TCR system performance. The former is discussed in Section Reforming system and exhaust gas available enthalpy and the latter – in Section System performance.

Please cite this article in press as: Poran A, et al., Direct injection internal combustion engine with high-pressure thermochemical recuperation – Experimental study of the first prototype, International Journal of Hydrogen Energy (2018), https://doi.org/10.1016/j.ijhydene.2018.04.190

Table 3 – Accuracy of measured data and uncertainty of calculated parameters.

Accuracy of measured parameters	
Device	Manufacturer, (Accuracy)
Crankshaft encoder 2613B	Kistler Instrument A.G., (Resolution 0.5°, Dynamic accuracy +0.02° at 10000 rpm)
Charge Amplifier Type 5018	Kistler Instrument A.G., (<±0.3% at 0–60 °C)
Water cooled pressure transducer 6061B	Kistler Instrument A.G., (Max. linearity ≤±0.29% FS[a])
BlueShadow P80 pump	Knauer, (±2% accuracy, 0.1% precision)
Air flow sensor VA420 with integrated measuring unit	CS Instruments GmbH, (±1.5% of MV[a])
Wide-band Lambda sensor LC-1 kit	Innovate Motorsports based on Bosch LSU 4.2 O_2 sensor, (at λ = 1: ±0.007; at λ = 1.7: ±0.05)
NO_x analyzer 200 EH	Teledyne Instruments, (±0.5% of MV[a])
HC analyzer 600 series	California Analytical Instruments, (±0.5% of FS[a])
CO, CO_2 analyzer 600 series	California Analytical Instruments, (±1% of FS[a])
Power gauge (Wattmeter) DW-6060	Lutron Electronics Company, (±1%)
Digital scales GF-12K	A&D Ltd, (±0.1 g)
Maximal uncertainty of calculated parameters	
IMEP	±5%
Indicated Power	±5%

[a] FS – full scale, MV – Measured value.

Reforming system and exhaust gas available enthalpy

It is important to make sure that the exhaust gases possess enough energy to sustain the endothermic fuel reactions and also make sure that the reformer and the HE utilize this energy efficiently. It is important whether unreformed primary fuel is injected into the engine (through bypass 36, Fig. 1) or separated from the flow in the separation tank (26, Fig. 1). Fig. 4 shows calculation results of the reformate normalized added enthalpy ($\overline{h}_{add}$) as a function of conversion (f) and HE effectiveness (ε) for both studied cases (with and without non-reformed fuel separation). ε and f values for seven experimental points shown in Fig. 4 were calculated based on the measured composition using Eqs. (7) and (9). The background surface ($\overline{h}_{add}$) was calculated for various values of $\varepsilon$and f according to Eq. (5) assuming MSR (Eq. (1)) reaction only and the following typical temperatures: (i) hot reforming products at HE inlet (point 3 in Fig. 3.) – 623 K; (ii) MWM at HE inlet (point 1 in Fig. 3) – 298 K.

The results presented in Fig. 4 show the great difference in the fraction of exhaust gas energy required for reforming between the cases with and without injection of the unreformed primary fuel. Evidently, in the complete methanol conversion case ($f = 1$), the reforming normalized added enthalpy value is the same but as conversion deteriorates, the difference becomes significant (4–5% for $f = 0.75$ and $0.5<\varepsilon < 1$). Also, it should be noticed that for the same reformate normalized added enthalpy, low conversion causes a reduction in the HE effectiveness (Fig. 4) because there is more condensable material in the reformate leading to higher heat load in the HE due to condensation and its related latent heat.

For each of the experimental points shown in Fig. 4, the available exhaust gas enthalpy was calculated (based on Eq. (7)) and is presented in Fig. 5.

The calculation was performed based on the measured reformate fuel composition and the reformer exhaust gas inlet and outlet temperatures. For generalization, these points are plotted on a graph with contour lines that were computed based on the assumption of MSR reaction only and the reformer outlet exhaust gas temperature 503 K (the experimentally measured data average for a 50 bar injection pressure). The point numbers correspond to those in Table 2. For all experimental points, $\overline{h}_{av}$ was higher than $\overline{h}_{add}$. Note that employing the $\overline{h}_{av}$ & $\overline{h}_{add}$-based approach is useful in real-time monitoring during the experiment of available exhaust gas enthalpy sufficiency for sustainable TCR operation. From Figs. 4 and 6 it may seem that for point #7 $\overline{h}_{av}<\overline{h}_{add}$. The reason is that the assumptions made in plotting the general background in Figs. 4 and 6 ($T_8 = 503$ K; $T_3 = 623$ K) don't fit well this operating mode (the measured T_8 ~ 473 K and T_3 ~ 540 K). At this regime, to reduce methanol condensation between the HE and injector and to enable better exhaust enthalpy usage, the injection pressure was lowered from 50 bar (employed in points 1-6) to 30 bar. This reduced the temperature of

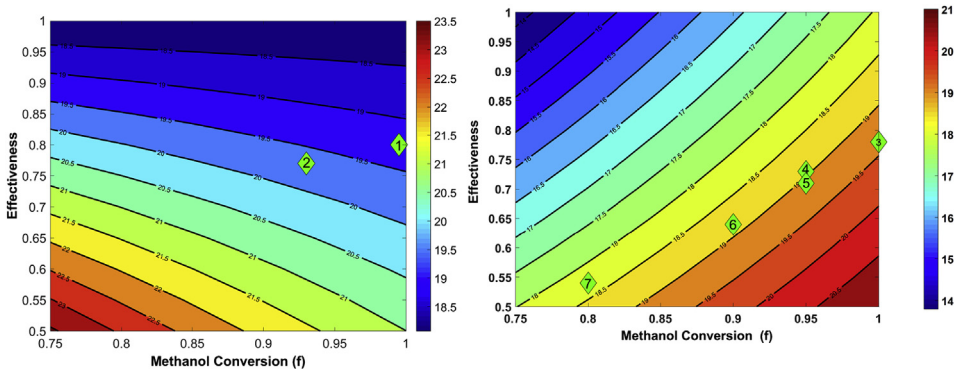

Fig. 4 – Reformate added enthalpy normalized by LHV of the gaseous reforming products (left) and total reforming products (right) as a function of methanol conversion (f) and HE effectiveness (ε). Numbers in the figure correspond to those of Table 2.

Please cite this article in press as: Poran A, et al., Direct injection internal combustion engine with high-pressure thermochemical recuperation – Experimental study of the first prototype, International Journal of Hydrogen Energy (2018), https://doi.org/10.1016/j.ijhydene.2018.04.190

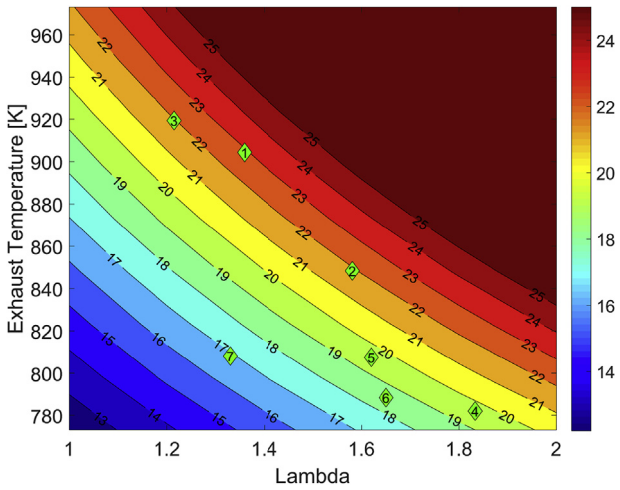

Fig. 5 – Normalized available exhaust gas enthalpy ($\bar{h}_{av}$) as a function of exhaust temperatures and Lambda. Numbers in the figure correspond to those of Table 2.

evaporation and subsequently – the MWM temperature at the cold side of the reformer and the exhaust gas outlet temperature (pts. 2 & 8 in Fig. 3, respectively). Moreover, to increase the temperature of exhaust gas (and subsequently – $\bar{h}_{av}$), the throttle was partially closed at this operation regime (Table 2). Fig. 6 shows the temperature distribution along the reformer axis for the seven steady-state regimes discussed above.

In the current TCR configuration (hot reformate is cooled before injection while preheating the MWM), the MWM starts evaporating in the HE, and hence enters the cold side of the reformer at its evaporation temperature (T_{ev}). Thus, the exhaust gas outlet temperature (down-bounded by the temperature at the cold side of the reformer – left side of Fig. 6) is actually bounded by the mixture evaporation temperature: $T_8 \geq T_2 = T_{ev}$. The experimental results show that indeed the temperature at the cold side of the reformer is very close to published MWM evaporation temperatures [34]. The increase in temperatures along the reformer also implies that the reaction rate is slower than the heat-transfer rate. The reason is that the reaction is diffusion-limited due to the relatively large size of catalyst pellets that were filled in the reformer tubes only by gravity forces (i.e. not mechanically pressed).

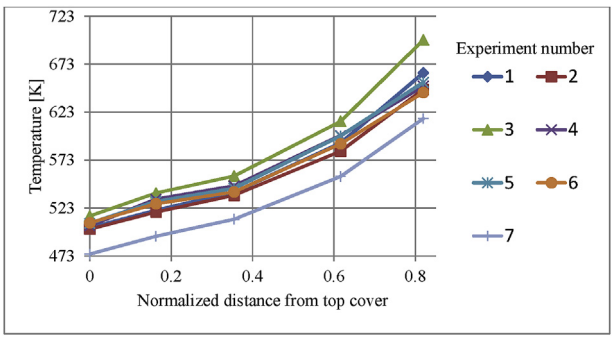

Fig. 6 – Temperature distribution along the reformer axis. Numbers in the figure legend correspond to those in Table 2.

According to experimental data of Artoul [35], for the employed catalyst pellet size, the effectiveness factor (ratio of the diffusion limited reaction rate to the reaction rate without diffusion limitations [36]) is about 0.35 at 503 K and 0.18 at 573 K. This means that reaction rate could at least be tripled by using catalyst pellets with radius 0.2 mm [35] or by applying more advanced catalyst coating technologies. This would increase the conversion (f), reduce the heat load of the HE and increase its effectiveness. The operating conditions of the HP-TCR system at various engine regimes are summarized in Table 4.

Some other approaches may be employed to improve waste heat recovery and conversion. It is possible to increase exhaust gas energy utilization by splitting the cold MWM flow (pt. 1 in Fig. 3) in such a way that a part of the primary fuel flows through the HE as in Fig. 3, and the rest is preheated in an additional heat exchanger by the exhaust gases leaving the reformer at temperature T_8. This adds complexity to the system but allows extracting more energy from the exhaust gas by cooling it below T_{ev}. A possibility to increase conversion by injecting the hot reformate to the engine without cooling it in the HE could be considered as well for some operating modes. This would increase exhaust gas temperature at the reformer inlet, prevent methanol condensation and allow achieving lower temperatures at the reformer outlet (because MWM would enter the reformer at ambient temperature). The negative aspects of this approach, like some increase in the compression work [26] and elevated heat losses should be taken into account. When the available waste energy is not enough to sustain endothermic fuel reforming reactions, a separate injection of some unreformed methanol may be considered. This would increase the HE effectiveness, the reformer temperatures and would finally lead to a higher usage of the reformed fuel compared to the case when the MWM just circulates in the system. An analysis of the suggested ways to improve waste heat recovery and conversion was out of the scope of this work.

The engine operation regime and the employed method of waste heat recovery affect the reforming temperature. The measured gaseous reforming products composition as a function of the reformer hot side temperature (most distant from the reformer top cover – Fig. 6) is shown in Fig. 7.

As showed by Poran et al. in the previous theoretical study [37], a higher CO fraction and respectively lower CO_2 and H_2 fractions in the reformate are expected with the reforming temperature increase, due to the reverse water gas shift reaction. The presence of methane was not expected at steam-to-methanol ratio = 1 [38]. Methane occurrence (in very

Table 4 – Operating conditions of the HP-TCR system.

Experiment No.	1	2	3	4	5	6	7
MWM temperature [K]	299	299	296	295	295	295	295
Pre-heated MWM temperature [K]	520	519	538	535	530	528	493
Hot reformate temperature [K]	660	643	696	605	598	584	539
Cooled reformate temperature [K]	370	368	387	373	377	384	385
Hot exhaust gas temperature [K]	903	850	919	782	807	788	808
Cooled exhaust gas temperature [K]	498	496	526	517	514	513	473

Please cite this article in press as: Poran A, et al., Direct injection internal combustion engine with high-pressure thermochemical recuperation – Experimental study of the first prototype, International Journal of Hydrogen Energy (2018), https://doi.org/10.1016/j.ijhydene.2018.04.190

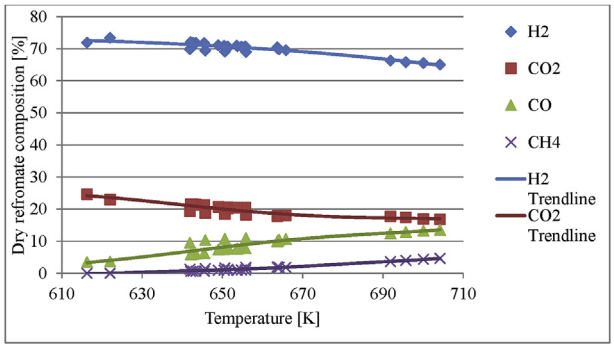

Fig. 7 – Dry reformate composition as a function of reformer hot side temperature.

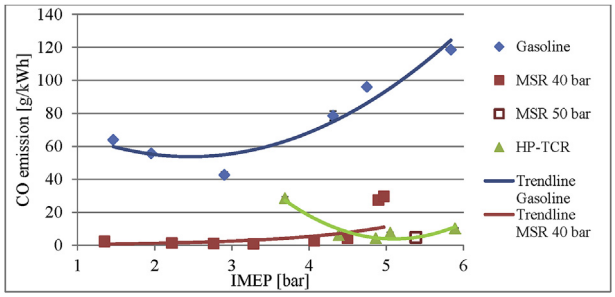

Fig. 8 – CO emissions comparison for gasoline, artificial MSR products, and HP-TCR system. The error bars show uncertainty for the calculated CO emission values.

small fractions) was a result of the excessively high reforming temperature exceeded the planned temperature range of 573–623 K. The high reforming temperature also resulted in higher than expected CO fraction. Higher CO and CH_4 fractions are beneficial for ICE with TCR since more exhaust heat is recovered and reformate with higher molar energy density is produced, which allows more flexibility in direct reformate injection [26]. Notably, the measured H_2 content in the reformate was ≥65% mol. at all investigated regimes and thus allowed exploiting the great advantages of H_2 combustion. When the temperature was in the expected range (573–623 K), H_2 content in the reformate was very close to the theoretical 75% of the MSR reaction (Fig. 7). The relatively high content of CO in the reformate together with the incomplete methanol conversion implies that the reformer suffers from diffusion limitation and possibly from unequal flow in its tubes. The latter results in elevated CO formation in the tubes with lower space velocity and higher residence time, as well as in reduced conversion in the tubes with higher space velocity and lower residence time. The performance of the high-pressure reforming system coupled with the previously studied DI-ICE [27–29] was investigated and is discussed in Section System performance.

System performance

Emissions and efficiency measurements of ICE with HP-TCR system were compared with baseline gasoline engine and performance of the same engine fed with artificially prepared MSR products from compressed gas cylinders. Fig. 8 shows the engine CO emissions.

As expected, the engine CO emissions with HP-TCR are much lower compared to the gasoline counterpart and lie in the same range with the artificial MSR. At the lowest investigated load (operation regime #7 of the ICE with HP-TCR), CO emissions increased significantly due to drops of condensed unreformed methanol that occasionally entered the cylinder through the injector and resulted in rich-mixture combustion. These methanol drops also caused increased HC emissions (Fig. 9).

The occasional intrusion of methanol drops to the combustion chamber roughly doubled or tripled the HC emissions compared to the case of artificial MSR products where lubricant was the only source of HC emissions. In the case of

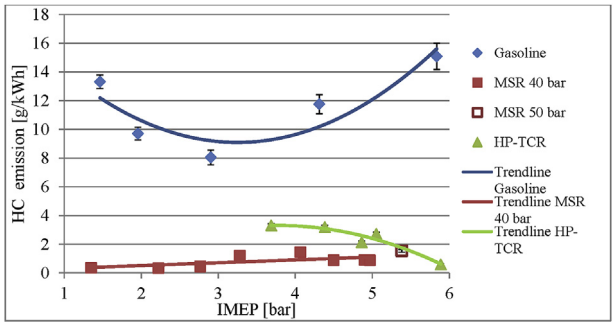

Fig. 9 – HC emissions comparison for gasoline, artificial MSR products, and HP-TCR system. The error bars show uncertainty for the calculated HC emission values.

complete conversion (highest load), the HC emissions remained the same as for artificial MSR products. This means that by further improvement of the high-pressure reforming system in one of the ways discussed above, CO and HC emissions of DI-ICE with HP-TCR can be significantly reduced. For NO_x, unlike the CO and HC emission cases, the HP-TCR system showed even better results than those of the artificial MSR (Fig. 10).

The low NO_x emissions of artificial MSR products and HP-TCR system are due to the lean-burn ability of the hydrogen-rich reformate and the CO_2 presence in methanol steam reforming products [27,28]. The latter is a diluent gas and when injected into the cylinder as a part of the reformate fuel,

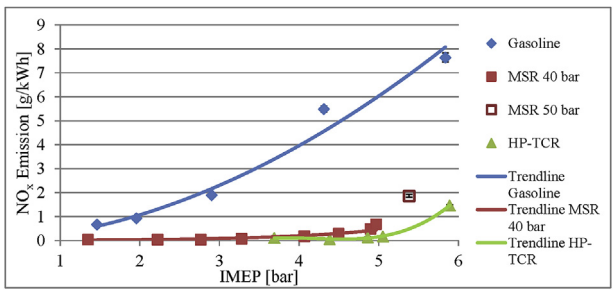

Fig. 10 – NO_x emissions comparison for gasoline, artificial MSR products, and HP-TCR system. The error bars show uncertainty for the calculated NO_x emission values.

Please cite this article in press as: Poran A, et al., Direct injection internal combustion engine with high-pressure thermochemical recuperation – Experimental study of the first prototype, International Journal of Hydrogen Energy (2018), https://doi.org/10.1016/j.ijhydene.2018.04.190

it reduces the combustion temperatures. In the case of HP-TCR, the NO_x emissions are even lower than with artificial MSR due to the presence of water in the injected reformate that further reduces the combustion temperatures and hence the NO_x formation.

Also in the case of CO_2 emissions, the HP-TCR showed significant improvement over gasoline case but slightly inferior results compared to artificial MSR products (Fig. 11).

Notably, some of the measured reduction in specific CO_2 emissions (~7%) originates from using a low carbon intensity primary fuel – methanol as compared to gasoline, while the rest comes from the improvement in fuel conversion efficiency. A comparison of the engine indicated efficiency for gasoline, artificial MSR products, and HP-TCR system is shown in Fig. 12.

HP-TCR shows great improvement in terms of efficiency compared to gasoline. From the previous experiments performed with DI of CH_4 [27], we can estimate that approximately 8% relative improvement in efficiency comes from retrofitting the gasoline carburetor engine with a DI injector. The rest of improvement results from the waste heat recovery, lean burn benefits and the improved reformate combustion properties. For HP-TCR the achieved efficiency gain is slightly inferior compared to artificial MSR products, especially at low load. There is less energy in the exhaust gases with engine load reduction which reduces the reforming system performance (lower conversion and lower HE effectiveness) and subsequently adversely affects the ICE with HP-TCR performance. As mentioned previously, lower conversion resulted in the sporadic intrusion of unreformed condensed methanol drops into the cylinder, which led to worsened combustion quality and a subsequent efficiency reduction. The results of the artificial MSR fueling may serve as a reference case to show how much improvement may be achieved by improving the reforming system. The range of improvement over gasoline achieved with HP-TCR system and compared with artificial MSR is shown in Table 5.

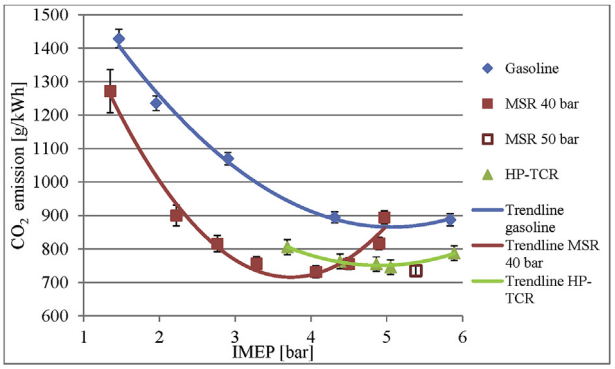

Fig. 11 – CO_2 emissions comparison for gasoline, artificial MSR products, and HP-TCR system. The error bars show uncertainty for the calculated CO_2 emission values.

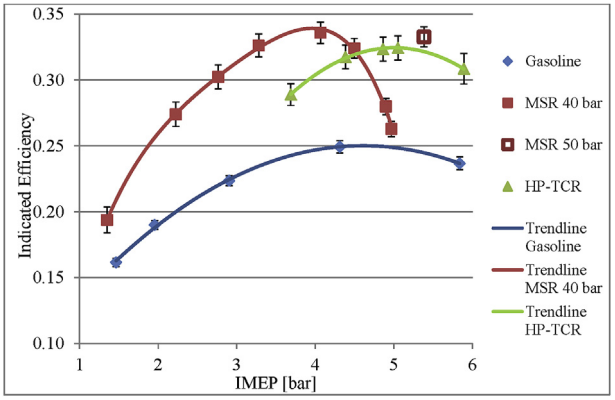

Fig. 12 – Indicated efficiency comparison of gasoline, artificial MSR products, and HP-TCR system. The error bars show uncertainty for the calculated indicated efficiency values.

Table 5 – Engine performance improvement range of artificial MSR, and HP-TCR over gasoline.

	Engine performance improvement range [%]	
	MSR	HP-TCR
Efficiency	18–39	19–30
CO	90–96	55–91
CO_2	10–25	11–15
HC	85–97	74–96
NO_x	73–94	81–97

As seen, although the system is not optimized yet, it shows a significant improvement over the gasoline reference case with 19%–30% increase in indicated efficiency and reduction in NO_x, CO, HC and CO_2 emissions by up to 97, 91, 96 and 15%, respectively. The results obtained for ICE fed with artificially prepared MSR reformate show even higher performance improvement that may be achieved. Note that the percentage efficiency improvement (19–30%) over ICE feeding with gasoline is higher than the reduction in CO_2 emissions (11–15%) because of carbon redistribution from CO and HC emissions to CO_2. When ICE is fueled with gasoline, the carbon supplied with the fuel is emitted as CO_2, CO, and HC. Whereas, for ICE with HP-TCR, CO and HC emissions are mitigated by up to 91% and 96%, respectively. Hence, the majority of carbon introduced with the fuel into the ICE is emitted as CO_2, thereby resulting in a lower reduction in CO_2 emissions relative to efficiency improvement.

Summary and conclusions

A need in substantial efficiency improvement of propulsion systems together with mitigation of their GHG and target pollutant emissions, as well as in use of renewable alternatives to fossil oil fuels were the main reasons that lead to the reported study.

This work reports for the first time the experimental study results of a novel approach – an internal combustion engine with High-Pressure Thermochemical Recuperation. The system employs methanol – a low-carbon-intensity alternative liquid primary fuel (enables convenient gasoline-like vehicle fueling), however the ICE burns hydrogen-rich methanol

Please cite this article in press as: Poran A, et al., Direct injection internal combustion engine with high-pressure thermochemical recuperation – Experimental study of the first prototype, International Journal of Hydrogen Energy (2018), https://doi.org/10.1016/j.ijhydene.2018.04.190

steam reforming products as a standalone fuel. The suggested concept allows eliminating the major drawbacks of the known TCR methods, like engine power loss and abnormal combustion. The experimental results discussed in the reported study of DI ICE with HP-TCR system is a significant step forward compared to the studies previously published by authors of the same engine fed by artificially prepared reformate, because the developed system is the first ever working prototype of ICE with HP- TCR which was investigated for the first time.

Although the system is not optimized yet, it demonstrates a significant performance improvement over the gasoline reference case with 19%–30% increase in indicated efficiency and reduction in NO_x, CO, HC and CO_2 emissions by up to 97, 91, 96 and 15%, respectively. The results of engine feeding with artificially prepared MSR products show the further improvement potential that may be achieved.

The achieved performance of ICE with HP-TCR shows a good prospect to continue the research towards an automotive-scale system development.

Despite the achieved significant gain in efficiency and emissions mitigation, the obtained results clearly show that HP-TCR system performance can be further improved. The reformer reaction rate is too slow and its speeding-up may allow reduction of the reformer size together with the increase of methanol conversion. For this purpose, reducing the catalyst pellet size in the reformer or applying a coated reformer type is suggested.

It is shown that reforming pressure reduction can enable better exhaust gas energy extraction. The pressure reduction can be achieved by increasing the injector flow area. Among other performance improvement options, further heat exchanger effectiveness increase, splitting the methanol-water mixture flow (where part of the mixture is preheated by the hot reformate and another part – by the exhaust gas) and injecting the reformate directly after the reformer at low-load regimes are mentioned.

Acknowledgements

The authors gratefully acknowledge the financial support of the Israel Science Foundation (grants 1728/12 and 2054/17); Israel Ministry of Environmental Protection (grant 133-1-5); Israel Ministry of National Infrastructures, Energy and Water Resources (grant 215-11-025); Israel Ministry of Science, Technology and Space; Wolfson Family Charitable Trust; Rieger Foundation and the Grand Technion Energy Program.

REFERENCES

[1] Tartakovsky L, Gutman M, Mosyak A. Energy efficiency of road vehicles – trends and challenges. Chapter 3 in the Edited Collection. In: Cavalcanti Emmanuel F Santos, Barbosa Marcos Ribeiro, editors. Energy efficiency: methods, limitations and challenges. Nova Science Publishers; 2012. p. 63–90. 2012.

[2] Al-Baghdadi MARS. Performance study of a four-stroke spark ignition engine working with both of hydrogen and ethyl alcohol as supplementary fuel. Int J Hydrogen Energy 2000;25(10):1005–9.

[3] Wang X, Ge Y, Zhang C, Tan J, Hao L, Liu J, et al. Effects of engine misfire on regulated, unregulated emissions from a methanol-fueled vehicle and its ozone forming potential. Appl Energy 2016;177:187–95.

[4] Nguyen DK, Verhelst S. Computational study of the Laminar reaction front properties of diluted methanol–air flames enriched by the fuel reforming product. Energy Fuel 2017;31(9):9991–10002.

[5] Shudo T, Shima Y, Fujii T. Production of dimethyl ether and hydrogen by methanol reforming for an HCCI engine system with waste heat recovery–continuous control of fuel ignitability and utilization of exhaust gas heat. Int J Hydrogen Energy 2009;34(18):7638–47.

[6] Casanovas A, Divins NJ, Rejas A, Bosch R, Llorca J. Finding a suitable catalyst for on-board ethanol reforming using exhaust heat from an internal combustion engine. Int J Hydrogen Energy 2017;42(19):13681–90.

[7] Chiriac R, Racovitza A, Podevin P, Descombes G. On the possibility to reduce CO_2 emissions of heat engines fuelled partially with hydrogen produced by waste heat recovery. Int J Hydrogen Energy 2015;40(45):15856–63.

[8] Boretti A. Stoichiometric H_2-ICE with water injection and exhaust and coolant heat recovery through organic Rankine cycles. Int J Hydrogen Energy 2011;36(19):12591–600.

[9] Stobart R, Wijewardane MA, Yang Z. Comprehensive analysis of thermoelectric generation systems for automotive applications. Appl Therm Eng 2017;112:1433–44.

[10] Chen J, Li K, Liu C, Li M, Lv Y, Jia L, et al. Enhanced efficiency of thermoelectric generator by optimizing mechanical and electrical structures. Energies 2017;10(9):1329–43.

[11] Pashchenko D. Thermodynamic equilibrium analysis of combined dry and steam reforming of propane for thermochemical waste-heat recuperation. Int J Hydrogen Energy 2017;42(22):14926–35.

[12] Kim J, Chun KM, Song S, Baek HK, Lee SW. The effects of hydrogen on the combustion, performance and emissions of a turbo gasoline direct-injection engine with exhaust gas recirculation. Int J Hydrogen Energy 2017;42(39):25074–87.

[13] Eyal A, Tartakovsky L. Reforming controlled homogenous charge compression ignition-simulation results. SAE Technical Paper; 2016. No. 2016-32-0014.

[14] Verhelst S. Recent progress in the use of hydrogen as a fuel for internal combustion engines. Int J Hydrogen Energy 2014;39:1071–85.

[15] Verhelst S, Wallner T. Hydrogen-fueled internal combustion engines. Prog Energy Combust Sci 2009;35:490–527.

[16] Tartakovsky L, Sheintuch M. Fuel reforming in internal combustion engines. Prog Energy Combust Sci 2018;67:88–114.

[17] Liao CH, Horng RF. Investigation on the hydrogen production by methanol steam reforming with engine exhaust heat recovery strategy. Int J Hydrogen Energy 2016;41(9):4957–68.

[18] Pettersson L, Sjostrom K. Decomposed methanol as a fuel—a review. Combust Sci Technol 1991;80(4–6):265–303.

[19] Thattarathody R, Sheintuch M. Kinetics and dynamics of methanol steam reforming on CuO/ZnO/alumina catalyst. Appl Catal Gen 2017;540:47–56.

[20] Nguyen DK, Verhelst S. Development of laminar burning velocity correlation for the simulation of methanol fueled SI engines operated with onboard fuel reformer. SAE Technical Paper; 2017. 2017-01-0539.

[21] Peppley BA, Amphlett JC, Kearns LM, Mann RF, Roberge PR. Hydrogen generation for fuel-cell power systems by high-pressure catalytic methanol-steam reforming. In: Energy

Please cite this article in press as: Poran A, et al., Direct injection internal combustion engine with high-pressure thermochemical recuperation – Experimental study of the first prototype, International Journal of Hydrogen Energy (2018), https://doi.org/10.1016/j.ijhydene.2018.04.190

conversion engineering conference, 1997. IECEC-97., Proceedings of the 32nd intersociety. IEEE; 1997, July. p. 831–6.
[22] Twigg MV, Spencer MS. Deactivation of copper metal catalysts for methanol decomposition, methanol steam reforming and methanol synthesis. Top Catal 2003;22(3–4):191–203.
[23] Marbán G, López A, López I, Valdés-Solís T. A highly active, selective and stable copper/cobalt-structured nanocatalyst for methanol decomposition. Appl Catal B Environ 2010;99(1):257–64.
[24] Matthias NS, Wallner T, Scarcelli R. A hydrogen direct injection engine concept that exceeds US DOE light-duty efficiency targets. SAE Int J Engines 2012;5:838–49.
[25] Tartakovsky L, Baibikov V, Veinblat M. Comparative performance analysis of SI engine fed by ethanol and methanol reforming products. SAE Technical Paper; 2013. No. 2013-01-2617.
[26] Poran A, Tartakovsky L. Energy efficiency of a direct-injection internal combustion engine with high-pressure methanol steam reforming. Energy 2015;88:506–14.
[27] Poran A, Tartakovsky L. Performance and emissions of a direct injection internal combustion engine devised for joint operation with a high-pressure thermochemical recuperation system. Energy 2017;124:214–26.
[28] Poran A, Tartakovsky L. Influence of methanol reformate injection strategy on performance, available exhaust gas enthalpy and emissions of a direct-injection spark ignition engine. Int J Hydrogen Energy 2017;42(23):15652–68.
[29] Tartakovsky L, Amiel R, Baibikov V, Fleischman R, Gutman M, Poran A, et al. SI engine with direct injection of methanol reforming products – first experimental results. SAE Technical Paper; 2015. No. 2015-32-0712.
[30] Chuahy FDF, Kokjohn SL. High efficiency dual-fuel combustion through thermochemical recovery and diesel reforming. Appl Energy 2017;195:503–22.
[31] Heywood JB. Internal combustion engine fundamentals. New York: McGraw-Hill; 1988.
[32] Moffat RJ. Describing the uncertainties in experimental results. Exp Therm Fluid Sci 1988;1(1):3–17.
[33] Brunt MF, Pond CR. Evaluation of techniques for absolute cylinder pressure correction. SAE Technical Paper; 1997. No. 970036.
[34] Teutenberg T, Wagner P, Gmehling J. High-temperature liquid chromatography. Part I. Determination of the vapour pressures of binary solvent mixtures—implications for liquid chromatographic separations. J Chromatogr A 2009;1216(37):6471–80.
[35] Artoul M. On-board hydrogen production by methanol steam reforming for internal combustion engine fueling (MSc Thesis). Haifa, Israel: Technion – Israel Institute of Technology; 2015.
[36] Chorkendorff I, Niemantsverdriet JW. Concepts of modern catalysis and kinetics. Weinheim: WILEY-VCH Gmbh & Co. KGaA; 2003.
[37] Poran A, Artoul M, Sheintuch M, Tartakovsky L. Modeling internal combustion engine with thermo-chemical recuperation of the waste heat by methanol steam reforming. SAE Int J Engines 2014;7:234–42.
[38] Choi Y, Stenger HG. Fuel cell grade hydrogen from methanol on a commercial $Cu/ZnO/Al_2O_3$ catalyst. Appl Catal B Environ 2002;38(4):259–69.

Please cite this article in press as: Poran A, et al., Direct injection internal combustion engine with high-pressure thermochemical recuperation – Experimental study of the first prototype, International Journal of Hydrogen Energy (2018), https://doi.org/10.1016/j.ijhydene.2018.04.190